Analysis of neural networks in subcortical visual structures using correlation methods

Andrzej T. Foik[a], Jan Popiołkiewicz[a], Katarzyna Żeber[a], Paulina Urban[a], Marek Bekisz[a], Andrzej Wróbel[a], Wioletta J. Waleszczyk*[a]
[a]Nenecki Institute of Experimental Biology, 3 Pasteur St. 02-093 Warsaw, Poland

*w.waleszczyk@nencki.gov.pl; phone +48 225892444; fax +48 228224352; www.nencki.gov.pl

ABSTRACT

Correlation methods were used to characterize the activity of single neurons and network connections in three subcortical structures of the cat visual system. Autocorrelation analysis performed on spike trains of single cells recorded from the lateral geniculate and perigeniculate nuclei showed the presence of bursts of high-frequency oscillations ranging from 100 to 550 Hz in their spontaneous activity. Autocorrelation performed on spike trains of single cells recorded from the superior colliculus also revealed oscillations, but in the frequency range of 10 - 90 Hz, both in the spontaneous and visually evoked neuronal activity. The presence of oscillations was confirmed with spectral analysis and a shift predictor was used to distinguish between stimulus-locked and stimulus-independent oscillations in visually evoked activities. Additionally, a crosscorrelation analysis performed on two spike trains recorded from the same electrode or pairs of electrodes in the superior colliculus, revealed a common input from an external source and the presence of inhibitory interactions in the neuronal network.

Keywords: brain, visual pathway, animal studies, neuronal activity, computational methods, spike train analysis

1. INTRODUCTION

The different methods used to study brain connectivity allow researchers to reveal anatomical links, functional connectivity (statistical dependences), and even causal interactions (effective connectivity) between distinct units within the nervous system[1]. Among the methods approaching the "connectivity problem", crosscorrelation analysis seems to be particularly important because this method, used to for spike trains recorded from single neurons located within the same or different structures, shows both anatomical and functional connectivity and allows us to determine the direction of information transfer and the effectiveness of the interneuronal connections[2,3,4]. The method is particularly suitable for examining the type of interactions (excitatory or inhibitory) between distinct units in the neural network and for revealing their common input[5]. We used a crosscorrelation analysis to study neuronal circuitry in subcortical structures of the visual system. Additionally, we also used another correlation method, the autocorrelation analysis, to examine the activity patterns of single neurons. The autocorrelation analysis can reveal oscillatory activity in a network, for example, the oscillation of cellular membrane potentials, or oscillations in the generation of spikes by a single neuron. Here we used these two methods to study neuronal activity in the thalamic and midbrain visual structures in order to demonstrate the usefulness of this approach to studying neural connectivity. More specifically, we analysed spike trains recorded from the dorsal lateral geniculate nucleus (dLGN) – the main relay nucleus transmitting visual information from the retina to the cortex, the perigeniculate nucleus – a group of inhibitory cells that gates dLGN activity by recurrent feedback input, and the superior colliculus (SC) – the first structure of the extrageniculate pathway, an alternative route for sending visual information to the cortex.

2. METHODOLOGY

Acute experiments were performed on anesthetized adult cats of either sex. All experimental procedures were carried out to minimize animal numbers and suffering, and followed the 2010/63/EU directive on the protection of animals used for

Photonics Applications in Astronomy, Communications, Industry, and High-Energy Physics Experiments 2014, edited by Ryszard S. Romaniuk, Proc. of SPIE Vol. 9290, 92901W

scientific purposes and the National Institutes of Health guidelines for the care and use of animals for experimental procedures. The experimental protocol was approved by the Local Ethics Committee at the Nencki Institute of Experimental Biology. The dLGN and PGN data were derived from previously published results[6] and reanalyzed for the present study.

2.1 **Surgical procedures**

Surgical procedures were performed according to standard methods described in detail elsewhere.[6,7] Briefly, cats were given dexamethasone phosphate (0.3 $mg \cdot kg^{-1}$, i.m.; Rapidexon, Eurovet Animal Health BV, Netherlands) to reduce brain oedema on the day preceding the experiment. Animals were initially anesthetized i.m. with a mixture of xylazine (3 $mg \cdot kg^{-1}$, i.m.; Xylavet, ScanVet), propionylpromazine (1 $mg \cdot kg^{-1}$, i.m. Combelen, Bayer), and ketamine (20 $mg \cdot kg^{-1}$, i.m.; Ketanest, BioVet). Tracheal and cephalic vein cannulations were performed to allow, respectively, artificial ventilation and infusion of paralyzing drugs. Anaesthesia was maintained with a gaseous mixture of N_2O/O_2 (2:1) and isoflurane (1 – 1.5 % during surgical procedures and 0.3 – 0.6% during recordings; Baxter, Poland). Antibiotics (enrofloxacin, 5 $mg \cdot kg^{-1}$, Baytril, Bayer Animal Health GmbH, Germany), dexamethasone phosphate (0.3 $mg \cdot kg^{-1}$), and atropine sulphate (0.1 $mg \cdot kg^{-1}$, to reduce mucous secretion, WZF Polfa S.A., Poland) were injected i.m. daily. Paralysis was maintained during experiments by a continuous infusion of gallamine triethiodide (7.5 $mg \cdot kg^{-1} \cdot hr^{-1}$, i.v.) in a mixture of equal parts of 5% glucose and sodium lactate. Body temperature was automatically maintained at ~ 37.5 °C with an electric heating blanket. Animals were artificially ventilated and expired CO_2 was continuously monitored and maintained between 3.5 – 4.5% by adjusting the rate and/or stroke volume of the pulmonary pump. The heart rate and the electrocorticogram (ECoG; occipital lobe) from the side contralateral to the recording site were monitored continuously. A heart rate below 220 beats $minute^{-1}$ and slow-wave synchronized cortical activity were maintained by adjusting the isoflurane level in the gaseous N_2O and O_2 mixture. Atropine sulphate (1-2 drops, 0.5% Atropinum Sulfuricum, WZF Polfa S.A, Poland) and phenylephrine hydrochloride (1-2 drops, 10% Neo-Synephrine, Ursapharm, Germany) were applied daily onto the corneas to dilate the pupils and retract the nictitating membranes. Air-permeable zero-power contact lenses were used to protect the corneas from drying. Lenses of other power were used if needed. A typical experiment lasted four days. During this time neuronal activity from subcortical and cortical visual structures was recorded.

2.2 **Signal recording**

Extracellular single unit recordings were made from neurons in the *stratum griseum superficiale*, *stratum opticum,* and the upper part of the *stratum griseum intermediale* of the SC, the dLGN, and the PGN. Action potentials were recorded with tungsten, stainless-steel (6-10 MΩ; FHC, Brunswick, ME), or platinum-iridium microelectrodes (1-2 MΩ; Thomas Recording GmbH, Germany), conventionally amplified, monitored *via* a loudspeaker, and visualized on an oscilloscope. A one (FHC, Brunswick, ME), 12, or 64 channel recording system was used (3 or 16 Electrode Eckhorn Matrix System with tetrode extension, Thomas Recording GmbH, Germany). Recorded signals were digitized and fed to a PC computer for on-line display, analysis, and data storage using CED 1401 Plus or Power 1401 mk II and Spike2 software (Cambridge Electronic Design, UK), or a data acquisition USB-ME256-System (Multichannel Systems, Germany). Signals containing spike waveforms were band-pass filtered between 0.5 - 5 kHz and digitized at a sampling rate of 50 kHz. The ECoG was band-pass filtered between 0.1 - 100 Hz and digitized at a sampling rate of 1 kHz. Neuronal responsiveness to visual stimulation and the eye of origin (ipsi- and/or contralateral) were determined and the excitatory receptive fields (minimum discharge fields) plotted using black or white hand-held stimuli. Ocular dominance was determined by listening to the neuronal responses *via* a loudspeaker (spikes converted to standard TTL pulses). The dominant eye was chosen for subsequent visual stimulation (with the other eye covered). If conditions allowed, i.e. the registered signal was stable with well-isolated single unit activity, responses were also recorded during stimulation of the non-dominant eye.

2.3 **Visual stimulation**

We recorded spontaneous activity and responses to a randomly placed flickering light rectangle (1 x 2 deg or 0.5 x 1 deg; 4 - 6 $cd \cdot m^{-2}$ stimulus luminance against a 0.5 - 1 $cd \cdot m^{-2}$ background luminance) or a moving light bar with a constant velocity ranging from 2 to 1000 $deg \cdot s^{-1}$ (velocity values were approximately uniformly distributed on a logarithmic scale). A slide projector under computer control was used to project stimuli onto a concave spherical screen located 0.75 m in front of the cat and covering a 70 deg area of the visual field. The centre of the screen was adjusted to overlap the recorded RF centre, and a constant velocity stimulus moved through the RF centre along its horizontal or vertical axis. Stimulus movement was achieved by a computer controlled rotation of a mirror attached to the axle of a galvanometer.

Voltage changes transferred to the galvanometer were generated by Spike2 software and a digital-analogue converter, CED 1401 Plus or Power 1401 mk II. To ensure smooth stimulus movement, a single sweep with a full 50 deg amplitude was achieved in 500 voltage steps for the fastest stimulus (1000 deg·s^{-1}) and up to 5000 steps for the slowest (2 deg·s^{-1}). Each trial consisted of motion in one direction followed by a 1 s pause and then motion in the reverse direction at the same velocity followed by 1 s pause. The number of trials was roughly proportional to stimulus velocity (10 repetitions for 2 deg·s^{-1} up to 100 repetitions for 1000 deg·s^{-1}).

3. DATA ANALYSIS

Data analyses was based on sets of neuronal spike trains of spontaneous (background) activity (lasting at least 60 s), spike trains recorded during repetitive stimulus motion, or spike trains obtained during stimulation with the flashing spot.

3.1 Spike sorting

Spike2 software was used for spike sorting (based on waveform analysis; Fig. 1B) and off-line conversion of single unit activity waveforms into discrete spike time occurrences. We analysed 122 out of a total of 168 SC units, for which we were sure that every spike was correctly classified during off-line sorting. In all cases, single unit discrimination was confirmed by the presence of an absolute refractory period in the interspike interval histogram (ISI; e.g. Fig. 1C).

Further data analyses were performed using Matlab software (The MathWorks Inc., Natic, MA).

3.2 Peri-stimulus time histogram

Peri-stimulus time histograms (PSTHs) were constructed based on the responses to all repetitions of a given stimulus; PSTH bin length was always 0.5 ms. In the following figures, the PSTH time bases were usually divided into 200 bins for ease of presentation regardless of the single trial duration. This approach resulted in different bin lengths that were dependent on stimulus velocity, but in no case did this change the characteristics of the presented response.

3.3 Correlation analysis

Autocorrelation

Raw autocorrelation histograms (rACHs; e.g. Fig. 1D) were computed following the method introduced by Perkel et al.[2,3] and Aertsen et al.[4] We used normalization similar to that proposed by Bair and coworkers[8] and Kohn and Smith.[9] The rACH computed for single spike trains was assessed according to the following equation:

$$rACH(\tau) = \frac{1}{M}\sum_{i=1}^{M}\frac{\sum_{t=1}^{N} x^i(t)x^i(t+\tau)}{(N-|\tau|)\lambda^i}, \qquad (1)$$

where M is the number of trials, N is the number of bins in the trial (the same in all trials), i is a given trial, τ - a time lag in the number of bins, λ is the mean spike count per bin in the i^{th} trial, and $x^i(t)$ is the spike train related to the i^{th} trial.

In the case of an averaged PSTH, $M = 1$, thus ACH for a PSTH was assessed according to the following simplification of equation 1:

$$ACH(PSTH)(\tau) = \frac{\sum_{t=1}^{N} x(t)x(t+\tau)}{(N-|\tau|)\lambda}, \qquad (2)$$

where N is the number of PSTH bins, $x(t)$ is the spike count in bin t of the PSTH, τ - particular time lag in the number of bins, and λ is the mean spike count per bin averaged over the whole PSTH.

rACHs were prepared from single spike trains or from PSTHs divided into 0.5 ms bins with a maximum lag of 0.3 s. To obtain a corrected ACH (cACH; e.g. Fig. 1F), a shift predictor (Equation 3; e.g. Fig. 1E) was computed and subtracted from the rACH to remove stimulus influences:

$$ShiftACH(\tau) = \frac{1}{M-1}\sum_{i=1}^{M-1}\frac{\sum_{t=1}^{N} x^i(t)x^{i+1}(t+\tau)}{(N-|\tau|)\sqrt{\lambda^i\lambda^{i+1}}} \quad . \tag{3}$$

Crosscorrelation

Raw crosscorrelation histograms (rCCHs) were computed and normalization was performed using similar methods to that detailed for rACHs[2,3,4,8,9] according to the following equation:

$$rCCH(\tau) = \frac{1}{M}\sum_{i=1}^{M}\frac{\sum_{t=1}^{N} x^i(t)y^i(t+\tau)}{(N-|\tau|)\sqrt{\lambda_1{}^i\lambda_2{}^i}}, \tag{4}$$

where M is the number of trials, N is the number of bins in the trial (the same in all trials), i is a given trial, τ - a time lag in the number of bins, $x^i(t)$ and $y^i(t)$ are the spike trains related to the i^{th} trial and $\lambda_1{}^i$ and $\lambda_2{}^i$ are the mean spike counts per bin in the i^{th} trial for spike train x and y, respectively.

To obtain corrected CCH (cCCH), a shift predictor (Equation 5) was computed and subtracted from the rCCH to remove stimulus influences:

$$ShiftCCH(\tau) = \frac{1}{M-1}\sum_{i=1}^{M-1}\frac{\sum_{t=1}^{N} x^i(t)y^{i+1}(t+\tau)}{(N-|\tau|)\sqrt{\lambda_1{}^i\lambda_2{}^{i+1}}} \quad . \tag{5}$$

3.4 **Fourier analysis**

Discrete Fourier transforms (DFT) were used to identify oscillation frequencies and were computed for both raw and corrected ACHs using a MatLab fft function (e.g. Fig. 1G and I).

4. **RESULTS**

Figure 1 shows a typical analyses performed for a recorded spike train. Spike waveforms were classified based on the principal component analysis. Inter-spike interval (ISI) histograms were computed to verify the correctness of the separation of single units by detecting the presence of a refractory period (Fig. 1C). The second peak in ISI indicated the oscillatory organization of the investigated spike train. The presence of oscillations in single unit activity was further confirmed using autocorrelation analysis (e.g. Figure 1D - F), and their frequencies were determined from the computed power spectra (Fig. 1 G - I). The crosscorrelation analysis was used to detect oscillations between two separate neurons in the network.

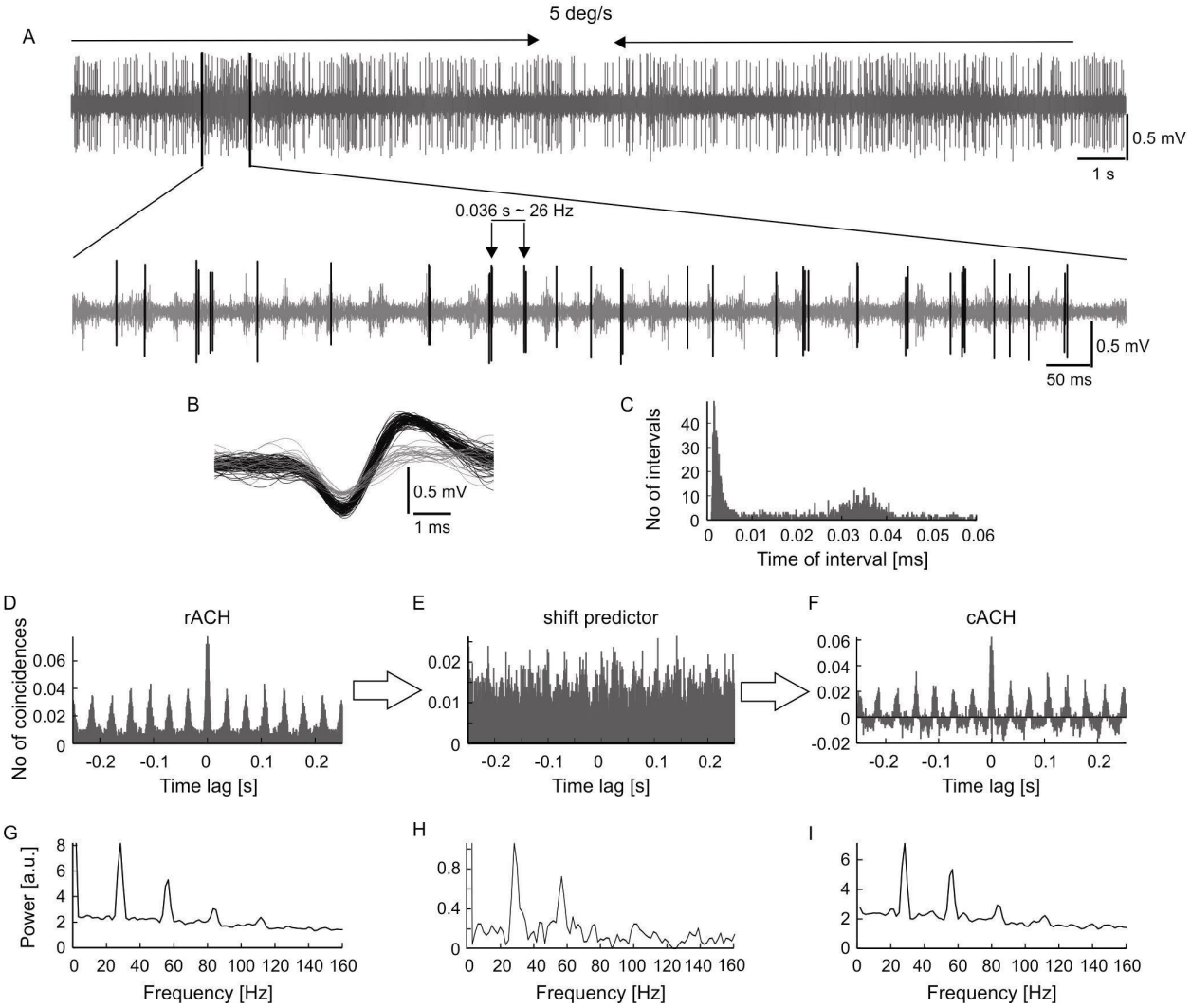

Figure 1. Extracellular neuronal recordings of oscillatory activity from the superficial layers of the SC. A, Top panel - the raw signal recorded in response to a light bar moving with velocity of 5 deg·s^{-1} back and forth through the receptive field of an investigated neuron. The panel placed just below represents an enlarged part of the raw signal. indicated by dashed lines. An oscillatory pattern of activity of a neuron with large amplitude spikes (black) is clearly represented by single spikes or spike-doublets appearing with a constant interval. The spikes of other, simultaneously recorded neurons are shown in grey. B, Spike waveforms selected from the spike train in A. C, Inter-spike interval (ISI) histogram for the unitary activity shown in A and B (large amplitude, black waveforms). The first peak reflects bursting frequency (seen in A as spike-doublets), the other peaks indicate oscillatory activity. D, Raw autocorrelogram (rACH) from the signal in A; resolution 0.5 ms. E, Shift predictor prepared from the same signal. F, Corrected autocorrelogram (cACH) obtained after subtraction of shift predictor in E from rACH in D. G - I, Power spectra calculated from the autocorrelograms in D - F.

4.1 **High-frequency oscillations in the LGN and PGN**

Neuronal activity in the thalamus appears in two modes: tonic, when neurons generate separate sodium-potassium action potentials, and bursting mode, when cells generate calcium spikes, which are the carriers for several high-frequency sodium-potassium action potentials. Figure 2 shows the results of autocorrelation analysis on a spike train with characteristic bursts obtained for a PGN neuron recorded in absence of visual stimulation (spontaneous activity). The extended part of the signal shows a typical high-frequency burst (Fig. 2B). Bursts were generated at a frequency of 1- 4 per second. An autocorrelogram with a short time lag obtained from the record shown in Figure

2B and the power spectra computed for this autocorrelogram reveal that the frequency of oscillations within the bursts ranged from 300 to 550 Hz (Fig. 2D). Spike frequencies recorded in LGN bursts were typically lower, in the range of 100 - 500 Hz.

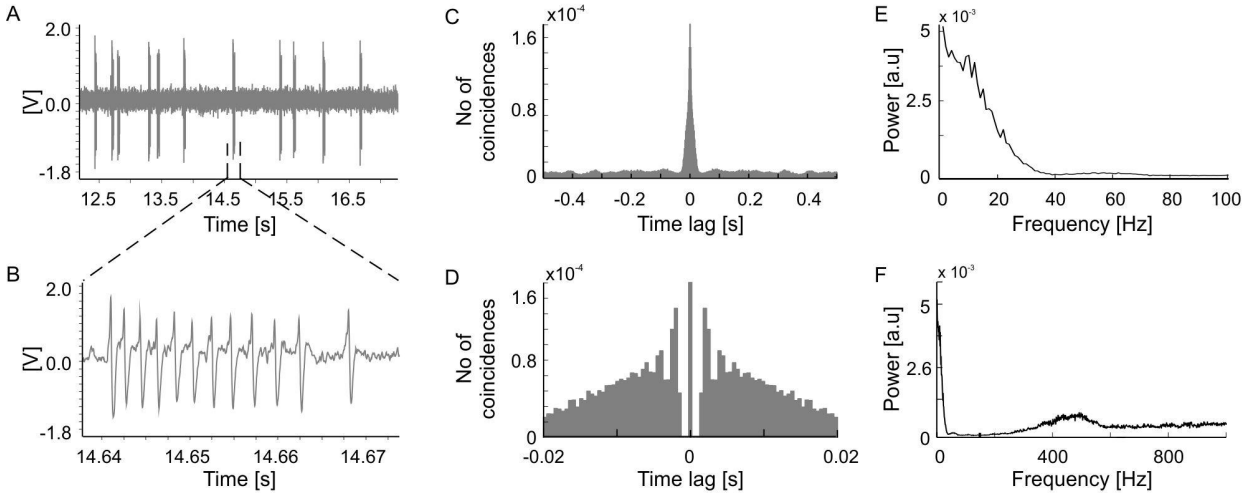

Figure 2. Autocorrelation analysis of a neuronal spike train recorded from the PGN. A, Raw signal recorded from a PGN neuron in absence of visual stimulation (spontaneous activity). B, A portion of the signal in A has been enlarged and shows a typical high-frequency burst. C and D, Autocorrelograms obtained from record shown in A with two time lags. E and F, Power spectra computed on the autocorrelograms shown in C and D.

4.2 **Oscillations in the spontaneous activity of SC cells**

Autocorrelations computed for single cell spike trains recorded from the SC also revealed oscillations, but these were in the frequency range of 10 - 90 Hz. Figure 3 shows examples of autocorrelation analyses performed for two spontaneously active SC neurons and reveals slow oscillations. Cells with spontaneous oscillations in the range of 60 - 70 Hz were characterized by relatively high activity (example in Fig. 3A and C).

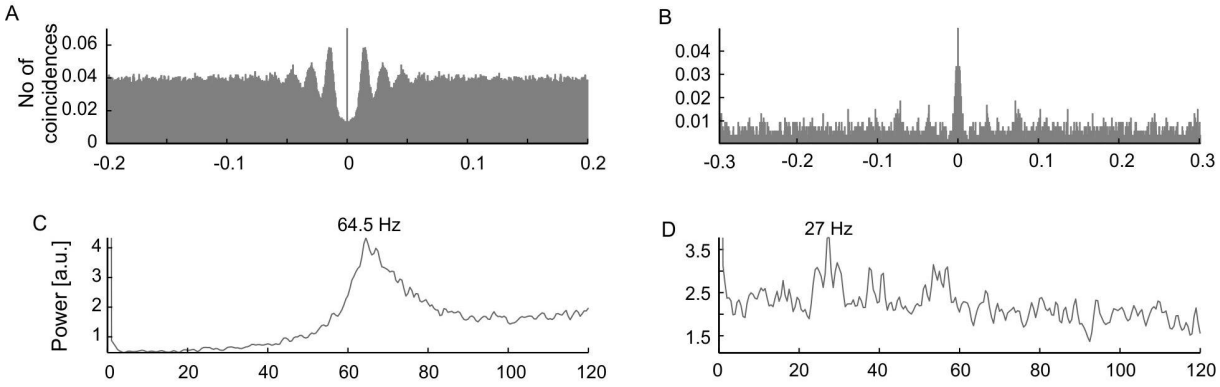

Figure 3. Oscillations in the spontaneous activity of SC neurons. The figure shows raw autocorrelograms (A and B) and the respective power spectra for the spontaneous activity of two SC neurons (C and D). Note the different oscillatory frequencies, 64.5 and 27 Hz, for the two cells.

4.3 **Oscillations in the evoked activity of SC cells**

Oscillations were also present in the visually evoked activity of SC cells. A typical example of SC cell responses to a light bar moving at low (20 deg·s^{-1}) and high (500 deg·s^{-1}) velocity can be seen in Figure 4. Stimulus phase-locked oscillations appearing with constant latency following stimulus onset were only present in responses to high velocity stimulations (Fig. 4B, D, F and H).

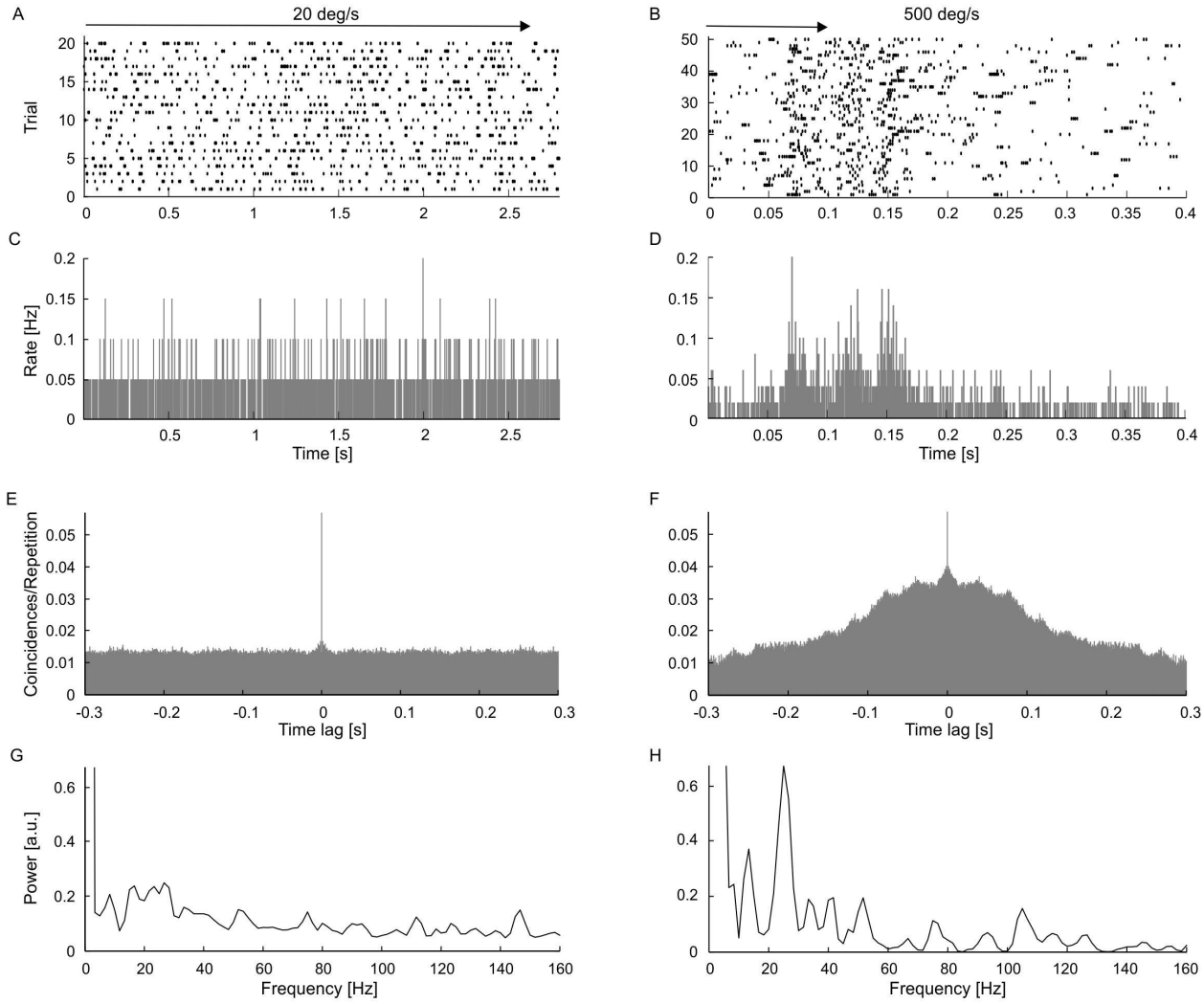

Figure 4. Stimulus velocity dependent oscillations in the activity of SC neuron. A, B, Raster plots for two velocities of stimulus movement: 20, and 500 deg·s^{-1} respectively. C, D, Corresponding PSTHs (800 bins). E, F, ACHs computed from the PSTH reveal the presence of stimulus phase-locked oscillations for high velocities. G, H, Amplitude spectra prepared from E, F. Note the changing temporal structure and increasing synchronization of the responses in the raster plots and PSTHs as stimulus velocity increases, which is confirmed in the power spectrum analysis.

We also identified oscillations in response to a flashing rectangular visual stimulus, as well as oscillations that were not related to the visual stimulation in any stimulus phase-dependent manner (not shown). These unrelated oscillations most likely represented spontaneous oscillations enhanced by visual stimulation.

4.4 **Crosscorrelation analyses in SC**

Crosscorrelation analyses were performed for simultaneously recorded activity of SC neurons by using the same electrode (closely adjacent cells) or tetrodes (bundles of four electrodes with recording tips separated by 300 μm). In majority of cases crosscorrelation analysis for pairs of SC neurons showed common, most likely retinal or cortical input. In rare cases interactions between SC neurons could be observed. In example presented in Figure 5 the crosscorrelation analysis revealed disynaptic inhibition between SC cells receiving common input.

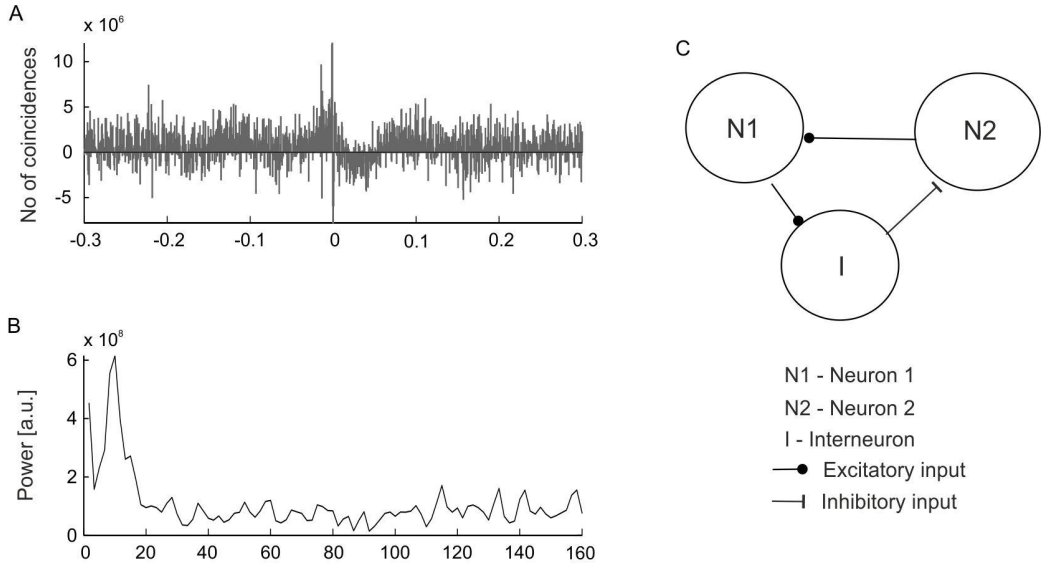

Figure 5. Crosscorrelation analysis of spiking activity for the pair of neurons recorded simultaneously from SC. A, Corrected crosscorrelogram (cCCH) showing type of interaction between two neurones in the SC. B, Power spectrum prepared from A confirming presence of 10 Hz oscillations in neuronal interactions. C, Schematic representation of the presumed interactions revealed by the cCCH shown in A.

5. **CONCLUSIONS**

We used correlation methods to study neuronal activity in the thalamic and midbrain visual structures. The autocorrelation analysis was used to examine the activity patterns of single neurons, while the crosscorrelation analysis to elucidate neuronal circuitry in subcortical structures of the visual system. We showed the usefulness of the autocorrelation method for revealing oscillatory activity in a network, and usefulness of the crrosscorrelation analysis for revealing presence of connections and type of interactions in the neuronal network.

5.1 **Usefulness of correlation analyses in optogenetic studies**

Optogenetic methods have emerged as powerful tools for identifying genetically-defined neuronal populations and for manipulation of their activity with exceptionally high temporal precision[10,11]. Optogenetics is used for dissecting neural network connectivity and to explore the function of different neuronal populations by controlling the activity in neural circuits[12,13] and animal behavior[14,15]. The first attempts integrated optogenetic manipulations of network activity with multichannel recording using silicon probes.[16] With a battery of correlation-based methods to study functional connectivity in neural circuits, such as used here, we are well equipped to tackle the task of exploring sensory networks using optogenetics, multichannel recordings and computational methods[17].

ACKNOWLEDGEMENTS

We thank Izabella Bednarska for excellent technical assistance and Thomas FitzGibbon for his comments on an earlier version of the manuscript. The work was supported by Polish National Science Centre grants N N303 820640 and 2013/08/W/NZ4/00691.

REFERENCES

[1] Sporns, O., "Brain connectivity," Scholarpedia, 2(10), 4695 (2007).
[2] Perkel, D.H., Gerstein, G.L. and Moore G.P., "Neuronal spike trains and stochastic point processes. I. The single spike train," Biophys. J 7, 391-418 (1967a).
[3] Perkel, D.H., Gerstein, G.L. and Moore G.P., "Neuronal spike trains and stochastic point processes. II. Simultaneous spike trains," Biophys. J 7, 419-440 (1967b).
[4] Aertsen, A.M., Gerstein, G.L., Habib, M.K. and Palm, G., "Dynamics of neuronal firing correlation: modulation of "effective connectivity,". J. Neurophysiol 61, 900-917 (1989).
[5] Ostojic, S., Brunel, N., Hakim, V., "How connectivity, background activity, and synaptic properties shape the cross-correlation between spike trains," J. Neurosci 29(33), 10234-10253 (2009).
[6] Waleszczyk, W.J., Bekisz, M. and Wróbel, A., "Cortical modulation of neuronal activity in the cat's lateral geniculate and perigeniculate nuclei," Exp. Neurol 196. 54-72 (2005).
[7] Mochol, G., Wójcik, D.K., Wypych, M., Wróbel, A. and Waleszczyk, W.J., "Variability of visual responses of superior colliculus neurons depends on stimulus velocity," J. Neurosci 30, 3199-3209 (2010).
[8] Bair, W., Zohary, E and Newsome, W.T., "Correlated firing in macaque visual area MT: time scales and relationship to behavior," J. Neurosci 21, 1676-1697 (2001).
[9] Kohn, A. and Smith, M.A., "Stimulus dependence of neuronal correlation in primary visual cortex of the macaque," J. Neurosci 25, 3661-3673 (2005).
[10] Boyden, E.S., Zhang, F., Bamberg, E., Nagel, G. and Deisseroth, K., "Millisecond-timescale, genetically targeted optical control of neural activity," Nat. Neurosci 8(9), 1263-1268 (2005).
[11] Deisseroth, K., "Optogenetics," Nat. Methods 8(1), 26-29 (2011).
[12] Halassa, M.M., Siegle, J.H., Ritt, J.T., Ting, J.T., Feng, G. and Moore, C.I., "Selective optical drive of thalamic reticular nucleus generates thalamic bursts and cortical spindles," Nat. Neurosci 14(9), 1118-1120 (2011).
[13] Royer, S., Zemelman, B.V., Losonczy, A., Kim, J., Chance, F., Magee, J.C. and Buzsáki, G., "Control of timing, rate and bursts of hippocampal place cells by dendritic and somatic inhibition," Nat. Neurosci 15(5), 769-775 (2012).
[14] Huber, D., Petreanu, L., Ghitani, N., Ranade, S., Hromádka, T., Mainen, Z. and Svoboda, K., "Sparse optical microstimulation in barrel cortex drives learned behaviour in freely moving mice," Nature 451(7174), 61-64 (2008).
[15] Smith, K.S., Virkud, A., Deisseroth, K. and Graybiel, A.M., "Reversible online control of habitual behavior by optogenetic perturbation of medial prefrontal cortex," Proc Natl Acad Sci U S A 109(46), 18932-18937 (2012).
[16] Royer, S., Zemelman, B.V., Barbic, M., Losonczy, A., Buzsáki, G. and Magee, J.C., "Multi-array silicon probes with integrated optical fibers: light-assisted perturbation and recording of local neural circuits in the behaving animal," Eur J Neurosci. 31(12):2279-91 (2010).
[17] Wróbel, A., Radzewicz, C., Mankiewicz, L., Hottowy, P., Knapska, E., Konopka, W., Kublik, E., Radwańska, K., Waleszczyk, W.J. and Wójcik, D.K.,"Neuroengineering control and regulation of behavior," Proc. SPIE in this issue.